

Rapid and Effective Functionalization of Graphene Oxide by Ionic Liquid

Weibo Yan, Yi Huang*, Yanfei Xu, Lu Huang, and Yongsheng Chen*

Key Laboratory of Functional Polymer Materials and Center for Nanoscale Science and Technology,
Institute of Polymer Chemistry, College of Chemistry, Nankai University, Tianjin 300 071, China

Functionalized graphene oxide (DDIB-GO) sheets, which can be homogeneously distributed into *ortho*-dichlorobenzene, were obtained via rapid and effective covalent functionalization with imidazolium ionic liquids (1,3-didodecylimidazolium bromine) through ion exchange. The resulting DDIB-GO sheets were characterized by Fourier transform infrared spectroscopy (FTIR), UV Vis NIR spectroscopy, X-ray photoelectron spectroscopy (XPS), thermal gravimetric analysis (TGA), transmission electron microscopy (TEM), Atomic force microscopy (AFM). Furthermore, FTIR, XPS and TGA show that the 1,3-didodecylimidazolium have been covalently attached to the GO sheets. UV Vis NIR, TEM, and AFM demonstrate that after functionalization, the size and shape of DDIB-GO sheets had little change compared with GO sheets and it was mostly dispersed in single layer. And good electronic conductivity of the film prepared from DDIB-GO in ODCB was obtained after high temperature annealing.

Keywords: Graphene Oxide, Ionic Liquid, Functionalization, Ionic Interactions, Conductivity.

1. INTRODUCTION

Graphene, with an atomically thin, 2-dimensional structure that consists of sp^2 -hybridized carbons, has attracted enormous interest in the area of solid state electronics^{1–4} and composite materials^{5–12} due to its fascinating electronic and mechanical properties. So far, the chemical reduction of exfoliated graphite oxide (GO) appears to be a more feasible fabrication technique for mass production of reduced graphene sheets.^{13–17} However, improving the dispersibility of GO or graphene in solution especially in nonpolar organic solvents and tailoring its electronic properties at the solid state are the biggest challenges in the practical applications.^{15, 18, 19} To overcome the first obstacle, so far, many methods have been focused on the non-covalent functionalization through van der Waals forces or π - π interactions,^{20–24} or covalent functionalization by reaction with epoxy,^{25, 26} hydroxyl groups,²⁷ and conjugated carbon atoms on the basal plane of GO,^{28–30} as well as the carboxyl acids decorating the edges of GO.³¹ However, noncovalent functionalization could introduce foreign stabilizers, sometimes affecting the coupling between the graphene sheets and the surrounding matrix, undesirable for many applications.^{32, 33} The covalent functionalization on the basal plane would create defects

on the graphene sheet, leading to the poor electronic properties.^{29, 34} Consequently, there is an urgent need for the development of a facile and efficient approach to produce large-scale processable GO sheets in nonpolar organic solvents such as *ortho*-dichlorobenzene (ODCB). This would further broaden the scope of applications, such as graphene-based organic and polymer composite materials or organic electronics utilizing graphene sheets as active layers and graphene-based chemistry reaction in nonpolar medium, as well as allowing for subsequent chemical functionalization.^{30, 35}

While carboxyl groups of GO are mainly distributed on the edge, so its functionalization would have little effect on the surface properties of GO or graphene, especially through small molecular, which is more economical and applicable. Common small molecular functionalized GO sheets could hardly produce good disperse and long-term stable in non-polar organic solvents. However, imidazolium ionic liquids (ILs) with charge, long chain alkyl and aromatic nucleus have good solubility in ODCB. So modification with ILs should enable the preparation of good and long-term stable disperse of functionalized GO sheets (ILs-GO) in ODCB by repulsion between charges and solubilizing effect of long chain alkyl.³⁵

Similar methods for dispersion of GO in organic solvents by ILs have been reported by Klaus Müllen et al.³⁵ and Suh et al.³⁶ But functionalized GO obtained by

*Authors to whom correspondence should be addressed.

Klaus Müllen et al. tended to disperse well in polar organic solvent such as chloroform. And functionalized GO obtained by Suh et al. was through noncovalent interactions between GO sheets and ionic liquid polymers (PIL) and by exchange of the hydrophilic anions and hydrophobic anions in the PIL. It tended to disperse well in polar aprotic solvents.

In this report, we describe a simple, rapid and effective method for the production of GO sheets dispersed in nonpolar organic solvent, ODCB by small molecule, imidazolium ionic liquids, which react with carboxyl groups by ion exchange. Subsequently, the conductivity of films prepared by the solution of ILs-GO in ODCB was tested.

2. EXPERIMENTAL DETAILS

2.1. Materials

Graphite was obtained from Qingdao Huarun Graphite Co. 1-Bromododecane was obtained from J & K Chemical Limited. Imidazole, 1-methylimidazole and 1-methyl-3-butylimidazolium bromine were obtained from Alfa Aesar. Graphene oxide was prepared using a modified Hummers method.³⁷ 1-methyl-3-dodecylimidazolium bromine (MDIB)³⁸ and 1,3-didodecylimidazolium bromine (DDIB)³⁹ were prepared using procedures reported in the literatures, respectively. All manipulations were carried out under a dry argon atmosphere using standard Schlenk techniques, and solvents were purified by standard procedures. ¹H NMR spectra were recorded on a Bruker AC-300 spectrometer. Chemical shifts, δ , are reported in ppm relative to the internal standard TMS. Mass spectra were recorded on a LCQ Advantage spectrometer with ESI resource. HRMS were recorded on a VG ZAB-HS mass spectrometer with ESI resource.

2.2. Preparation of 1-Methyl-3-Dodecylimidazolium Bromine (MDIB)

1-Bromododecane (15.00 g, 60 mmol) was added to a 1,4-dioxane (70 mL) solution of 1-methylimidazole (4.10 g, 50 mmol), and then the mixture refluxed at 130 °C for 24 hours under argon. The reaction mixture was cool, and evaporated under reduced pressure to remove solvent, then obtained light yellow oil. The oil was pour into ether (100 mL), white solid precipitated, filtered, washed with ether, then dried under vacuum for 12 hours to obtain white solid 15.60 g, yielded 94%. δ_{H} (300 MHz; CDCl₃; Me₄Si): 10.30 (1H, s), 7.54 (1H, d, $J = 1.5$ Hz), 7.40 (1H, d, $J = 1.2$ Hz), 4.32 (2H, t, $J = 7.2$ Hz), 4.14 (3H, s), 1.915 (2H, m), 1.33–1.25 (18H, m), 0.88 (3H, t, $J = 6.3$ Hz); m/z (ESI): 251.53 (MDIB⁺). HRMS (ESI) calcd for (MDIB)⁺: 251.2482; found: 251.2476.

2.3. Preparation of 1,3-Didodecylimidazolium Bromine (DDIB)

50% NaH (3.34 g) was slowly added to a DMF (60 mL) solution of imidazole (3.94 g) under argon for 20 min, and the mixture was stirred at ambient temperature for 4 hours, then added 1-Bromododecane (20.24 g) slowly for 20 min. The reaction mixture was stirred at 60 °C for 16 hours, poured into ice water, and then extracted by ethyl acetate (3 × 50 mL). Organic phase was dried by anhydrous magnesium sulfate, filtered, evaporated under reduced pressure to remove solvent, and obtained light oil.

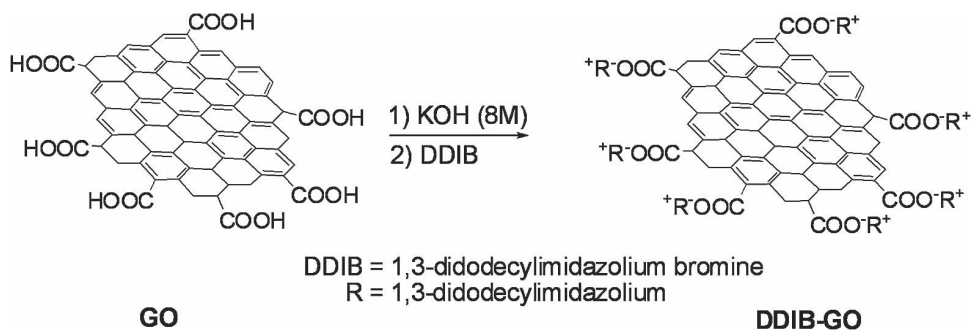
The light oil was added to a 1,4-dioxane (60 mL) solution of 1-Bromododecane, and then the mixture refluxed for 24 hours under argon. The reaction mixture was cool, and evaporated under reduced pressure to remove solvent, then obtained light yellow oil. The oil was pour into 100 mL ether/petroleum (1:2), washed with (3 × 50 mL) ether/petroleum (1:2), then dried under vacuum for 12 hours to obtain white solid 21.56 g, yielded 92%; δ_{H} (300 MHz; CDCl₃; Me₄Si): 10.38 (1H, s), 7.46 (1H, d, $J = 6.9$ Hz), 7.40 (1H, d, $J = 6.0$), 4.35 (4H, m), 1.91 (4H, m), 1.31–1.23 (36H, m), 0.88–0.86 (6H, m). m/z (ESI): 406.17 (DDIB⁺); HRMS (ESI) calcd for (DDIB)⁺: 405.4203; found: 405.4205.

2.4. Preparation of Graphene Oxide Sheets

Graphene oxide was prepared using a modified Hummers method.³⁷ Briefly, a small amount of flake graphite was vigorously stirred for 5 days in a solution of NaNO₃ and KMnO₄ in concentrated H₂SO₄, washed with 5 wt% H₂SO₄ in water and reacted with a 30 wt% aqueous solution of H₂O₂ to complete the oxidation. Inorganic anions and other impurities were removed through 15 washing cycles that included centrifugation, discarding supernatant liquid, and resuspending the solid in an aqueous mixture of 3 wt% H₂SO₄ and 0.5 wt% H₂O₂ using stirring and ultrasonication. Another set of centrifugation and washing procedures was effected three times using 3 wt% HCl in water as the dispersion medium and then one more time using purified water to resuspend the solids. This suspension was passed through a weak basic ion-exchange resin (Styrene-DVB D301T, Tianjin Nankai Hecheng S&T Co, Ltd.) to remove remaining acid. Finally the material was dried to obtain a loose brown powder which can be stored indefinitely.

2.5. Preparation of ILs-Functionalized Chemically Converted Graphene Oxide Sheets

As demonstrated in Scheme 1, the aqueous solution of GO (1 mg mL⁻¹) (PH = 9) with negative charges (COO⁻) are added to the solution of ILs (8 mg mL⁻¹) (1-methyl-3-butylimidazolium bromine (MBIB), 1-methyl-3-dodecylimidazolium bromine



Scheme 1. Synthesis route of DDIB-functionalized graphene oxide.

(MDIB), 1,3-didodecylimidazolium bromine (DDIB)) in ODCB, followed by shaking. The functionalization of GO takes place through ionic interactions.³⁵ To verify the feasibility of this method of functionalization, we amplified the reaction. GO (100 mg) was dispersed in deionized water (30 mL), then 8M KOH in H₂O (0.4 mL) was added to adjust pH value of the solution to ca. 9. The solution was stirred for 5 hours at ambient temperature, then DDIB (800 mg) in ODCB (60 mL) was added. After being stirred for 48 hour at ambient temperature, the mixture was allowed to stand for 1 hour to separate into two layers. The organic phase was separated and centrifuged, washed with CH₂Cl₂ and then dried under vacuum.

the organic phase. In contrast, the use of MDIB bearing one long alkyl substituent did not allow an efficient transfer from the water phase, while MDIB-functionalized GO showed poor solubility in water and aggregated at two-phase interface of water and ODCB. This finding indicated that the better solubility of DDIB in ODCB compared to MBIB and MDIB was crucial. Because of DDIB containing two didodecyl, DDIB-functionalized GO have better solubility than MBIB-functionalized and MDIB-functionalized GO in ODCB, and DDIB-functionalized GO was more easily transferred to the ODCB. Moreover, 1,3-didodecylimidazolium carrying positive charge are attached onto the edge of these GO sheets, and the repulsion between charges between GO sheets prevents

2.6. Measurement and Characterization

Transmission electron microscopy (TEM, FEI, TECNAI-20), atomic force microscope (AFM, Nanoscope IV, Digital Instruments, Veeco) were used to characterize the size and morphology of the samples. XPS spectra were recorded using a Kratos Axis Ultra DLD spectrometer employing a monochromated Al-K α X-ray source ($h\nu = 1486.6$ eV), hybrid (magnetic/electrostatic) optics and a multi-channel plate and delay line detector (DLD). Fourier transform infrared spectroscopy (FT-IR) spectra were obtained using a Bruker Tensor 27 spectrometer. All IR samples were prepared as pellets using spectroscopic grade KBr. UV vis NIR spectra were obtained with a Jasco V-570 spectrometer, and UV vis spectra were recorded on a Varian Cary 300 spectrophotometer. Thermal gravimetric analysis (TGA) were used by Netzsch STA 409PC with heating rate of 5 °C min⁻¹ from room temperature to 1000 °C under N₂.

3. RESULTS AND DISCUSSION

As demonstrated in Figure 1, apparently, in the NON, none ILs was added and the GO remained in the water phase because of the poor dispersion of GO in ODCB. MBIB-functionalized GO also remained in the water phase, whereas most DDIB-functionalized GO are transferred to

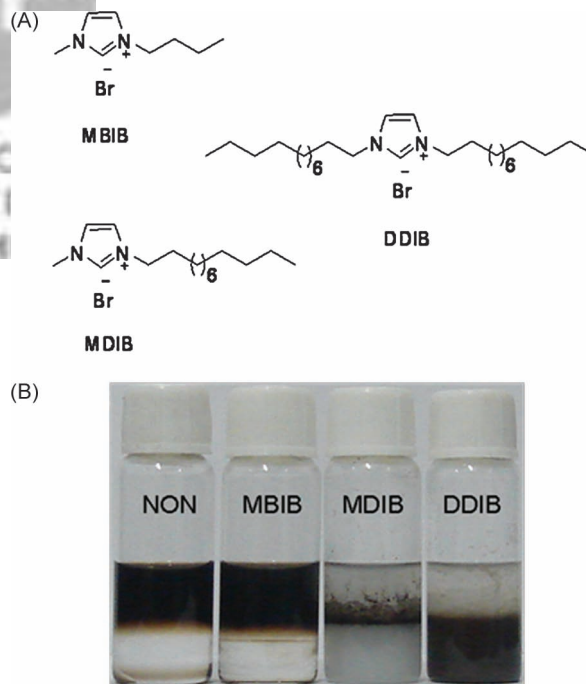


Fig. 1. (A) Chemical structure of three imidazolium ionic liquids used in this work. (B) Images of GO dispersion in water and ODCB cosolvents containing none ILs (NON), the imidazolium ionic liquids MBIB, MDIB, DDIB; parallel experiments were conducted using GO (1 mg mL⁻¹, 2 mL H₂O solution), ILs (8 mg mL⁻¹, 2 mL ODCB solution), pH = 9.

aggregation and leads to the stable dispersion of ILs-GO in ODCB.²⁰

Apart from the rational selection of suitable ILs molecules, the influence on the transfer efficiency of other experimental parameters, such as pH value, weight ratio between GO and ILs, and solvent (as shown in Fig. 2) have been investigated. A pH value around 9 and a weight ratio between GO and DDIB of around 1:8 were found to be the best conditions. Also, similar results were obtained by using CHCl_3 . But dichloromethane and toluene did not allow an efficient transfer process.

In amplified reaction, we obtained the same result as shown in Figure 1(B). The solid of DDIB-functionalized GO by centrifugation could re-disperse in ODCB. The maximum solubility of DDIB-GO was 1.3 mg mL^{-1} in ODCB.

Figure 3 shows the FTIR spectra of DDIB, GO, DDIB-GO. The FTIR spectra of GO conformed $\text{C}=\text{O}$ in

carboxylic acid moieties with strong stretching vibration at 1730 cm^{-1} .⁴⁰ The peak located at 1621 cm^{-1} could be ascribed to the skeletal vibration of graphitic domains.³⁵ While for DDIB-GO, the band of carboxylic acid vibration at 1730 cm^{-1} greatly decreased in intensity, while two new peaks appeared at 1570 cm^{-1} and 1419 cm^{-1} , which is ascribed to the asymmetric and symmetric vibration of the COO^- group, respectively. In DDIB and DDIB-GO, the intense absorption peaks at 2960 cm^{-1} , 2926 cm^{-1} , 2853 cm^{-1} are attributed to the stretching vibration of $-\text{CH}_2-$ and $-\text{CH}_3$. Especially the more intense absorption peaks at 2926 cm^{-1} and 1461 cm^{-1} indicates that the amount of $-\text{CH}_2-$ is more than $-\text{CH}_3$.³⁸ The peak at 1160 cm^{-1} in the DDIB-GO is the bending vibration of the C-H on the imidazole ring, corresponding to the peak at 1163 cm^{-1} in the DDIB.²⁶ Furthermore, the peaks at 1563 cm^{-1} and 1643 cm^{-1} for DDIB are the stretching vibration of the $\text{C}=\text{N}$ and $\text{C}=\text{C}$ on the imidazole ring,

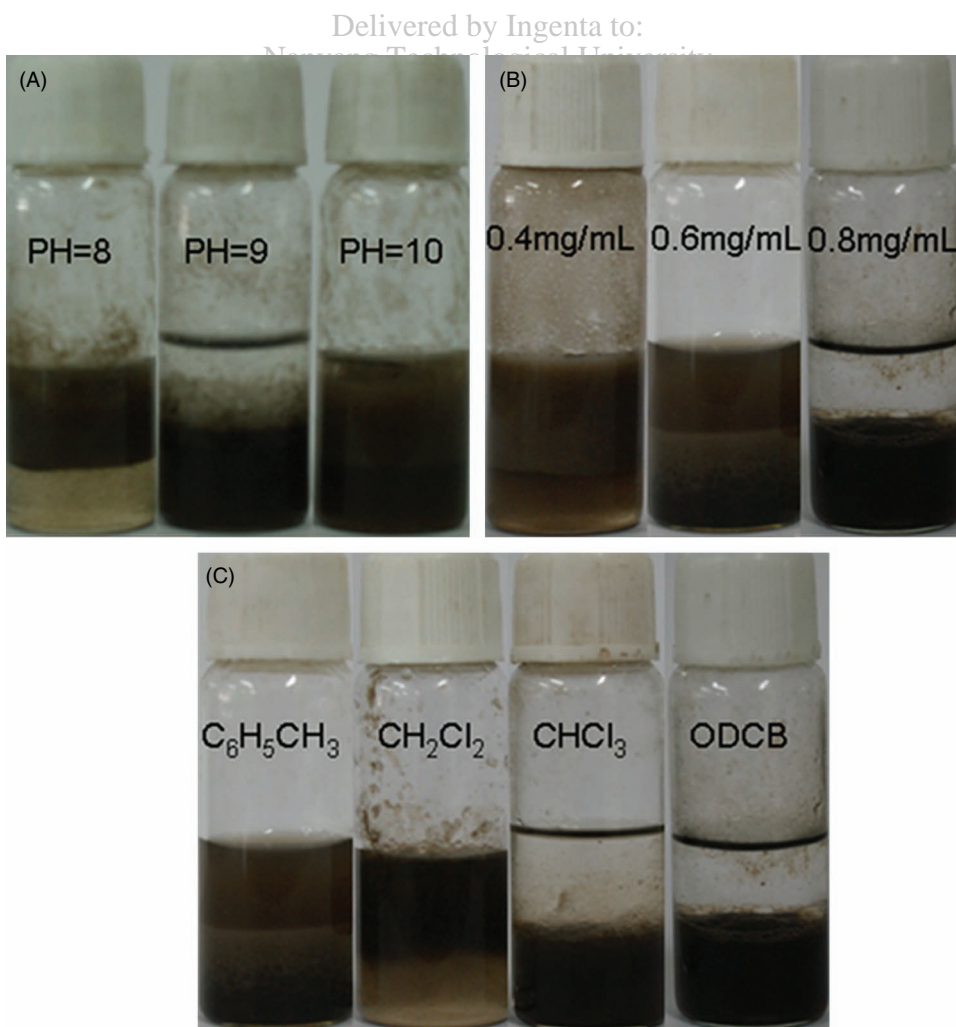


Fig. 2. Images of water and ODCB dispersion of DDIB functionalized GO (A) the effect of pH value: the parallel experiments were conducted using GO (1 mg mL^{-1} , $2 \text{ mL H}_2\text{O}$ solution), DDIB (8 mg mL^{-1} , 2 mL ODCB solution); (B) the effect of the effect of weight ratio between GO and DDIB: the parallel experiments were conducted using GO (1 mg mL^{-1} , $2 \text{ mL H}_2\text{O}$ solution), DDIB ($4, 6, 8 \text{ mg mL}^{-1}$, 2 mL ODCB solution) at $\text{pH} = 9$; (C) the effect of organic/water co-solvent category: the parallel experiments were conducted using GO (1 mg mL^{-1} , $2 \text{ mL H}_2\text{O}$ solution), DDIB (8 mg mL^{-1} , $2 \text{ mL C}_6\text{H}_5\text{CH}_3$, CH_2Cl_2 , CHCl_3 , ODCB solution) at $\text{pH} = 9$.

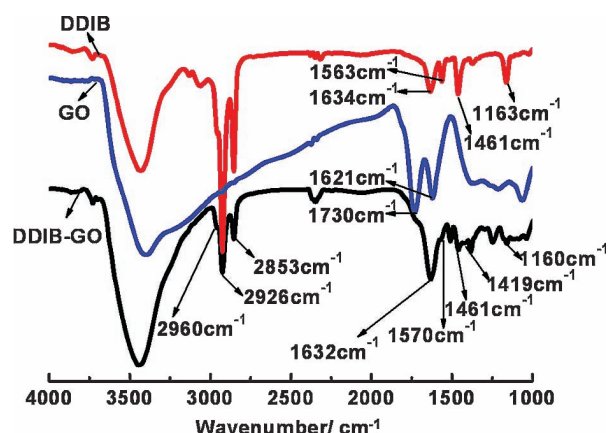


Fig. 3. FTIR spectra of DDIB, GO, DDIB-GO. The strong band at 2960 cm^{-1} , 2926 cm^{-1} , 2853 cm^{-1} , 1461 cm^{-1} , 1160 cm^{-1} arising from the C–H stretching vibration of the $\text{C}_{12}\text{H}_{25}$ -n, the asymmetrical and symmetrical stretching vibration of COO^- at 1570 cm^{-1} and 1419 cm^{-1} in the spectrum of DDIB-GO, indicates the DDIB is chemically attached to the GO sheets.

which is overlapped by the broad peak in the range of $1730\text{--}1534\text{ cm}^{-1}$ for DDIB-GO. Therefore, it is reasonable to conclude that most of many DDIB groups have been attached to the GO sheets by ionic interactions.

To further illustrate the successful functionalization by ion exchange, X-ray photoelectron spectroscopy (XPS) was performed on GO and DDIB-GO samples. Figure 4 shows the survey data of the solid samples and the higher resolution spectra of the N1s, O1s, and C1s areas, respectively. The survey (A) of GO shows the absence of any detectable amounts N1s (strongest XPS band is N1s usually found between 400 and 407 eV depending on the chemical environment). The survey XPS analysis of DDIB-GO shows an absence of any detectable amounts of K^{41} (the strongest XPS band is K2p, usually found between 290 and 297 eV) and any detectable amounts of Br (the strongest XPS band is Br3d, usually found between 65 and 85 eV), indicating that K^+ have been efficiently exchanged by DDIB^+ anions and meanwhile, K^+ and Br^- dissolves into the water phase. Moreover, the unreacted DDIB was also removed in the purification. And the C/O ratio of DDIB-GO is 74.71/21.51, which increased compared with that of GO, 64.61/34.67. The significant increasement of the ratio of C/O after functionalization indicated that the covalent functionalization of GO by DDIB successfully occurred. As shown in the inset of Figure 4(B), a strong band of N1s appears ca. 403.0 eV, with assigning to N–C.²⁶ Compared with GO, the survey of DDIB-GO shows the presence of N1s originating from DDIB with the C/N weight percentage 74.71/3.78, indicating that the covalent functionalization of GO by DDIB successfully occurred. Figure 3(C) shows O1s XPS spectra of GO (solid) and DDIB-GO (dotted). The O1s in GO appeared at ca. 530.98 eV, assigning to O in C–O–C, C–O–H and C=O. After interaction with

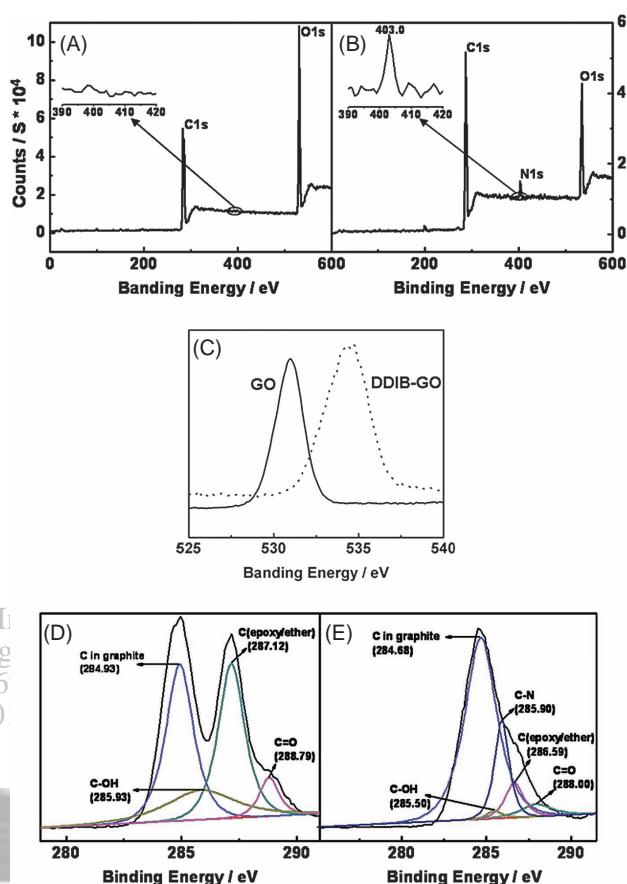


Fig. 4. The survey curves of (A) GO and (B) DDIB-GO, inset: the higher resolution curves of the N area. (C) The higher resolution curves of O1s area of GO (solid) and DDIB-GO (dotted). The higher resolution curves of C1s of (D) GO and (E) DDIB-GO.

DDIB, the O1s appeared at ca. 534.51 eV. The change is likely due to the change of banding energy for C=O. The higher resolution data of C1s area of the GO and DDIB-GO are shown in Figure 4(D) and (E), respectively. Figure 4(D) clearly indicates a considerable degree of oxidation with four components corresponding to carbon atoms in different functional groups: the C in graphite (BE, 284.93 eV), the C in C–OH (BE, 285.93 eV), the C in C–O epoxy/ether groups (BE, 287.12 eV), and the carbonyl C (BE, 288.79 eV). Figure 4(E) shows, for DDIB-GO, there is an additional component at 285.90 eV assigning to C bound to nitrogen,⁴² strongly indicating that the DDIB moieties react with the COOK groups on GO sheets. This is consistent with our FTIR analysis.

The successful functionalization of GO with DDIB was also reflected in TGA curves. As shown in Figure 5, the GO shows a large weight loss (30%) with an onset temperature at $201\text{ }^\circ\text{C}$, which can be attributed to the removal of the groups ($-\text{OH}$ and $-\text{COOH}$) from the GO sheets.⁴¹ The DDIB-GO shows the similar weight loss to GO below $200\text{ }^\circ\text{C}$, mainly the remove of adsorbed solvent, $-\text{OH}$. After $200\text{ }^\circ\text{C}$, DDIB-GO shows much slower weight loss, which indicates the strong charge interaction between DDIB^+ and

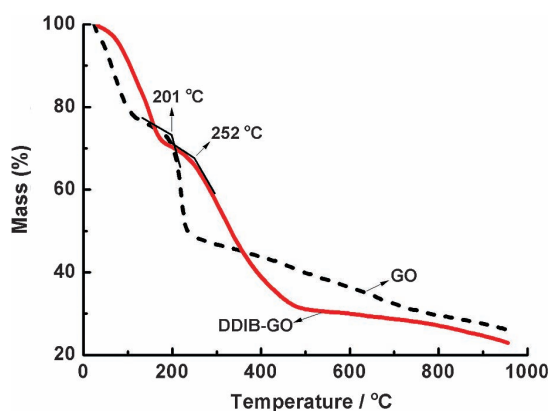


Fig. 5. TGA spectra of GO (dashed line) and DDIB-GO (solid line) obtained with a heating rate of 5 °C/min under purified nitrogen gas flow.

COO⁻ of on the edges of GO makes the COO⁻ more stable. And from 252 °C to 500 °C, DDIB-GO shows a large weight loss (37%) which can be attributed to the removal of the group of DDIB accompanied by COO⁻ from the GO sheets. Moreover, high temperature pyrolysis of DDIB-GO is similar to GO after 500 °C and attributed to pyrolysis of the carbon skeleton of graphene.⁴² These results demonstrate that after functionalization, DDIB-GO has better thermal stability than GO.

The prevention of aggregation is of particular importance for processability and applications of GO and graphene because most of its attractive properties are only associated with individual GO or graphene sheets. Solution-phase UV-Vis-NIR spectroscopy (Fig. 6) can be used to determine the solubility of DDIB-GO⁴³. The absorptions (at 295 nm) for the GO moiety¹⁵ were plotted against concentration and a good linear relationship was obtained with an R value of 0.999. Assuming the

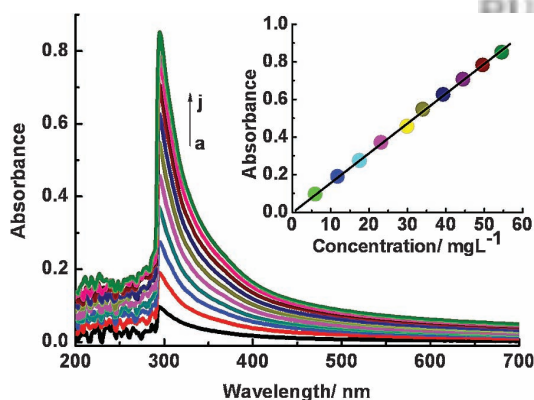


Fig. 6. Concentration dependence of UV absorption of DDIB-GO in ODCB (concentrations are 5.49, 11.76, 17.47, 23.08, 29.85, 33.96, 39.25, 44.44, 49.54, 54.54 mg L⁻¹ from a to j, respectively). Shown in the inset is a plot of optical density at maximal absorption position (295 nm) for the GO moiety versus concentration. The straight line in the plot in the inset is a linear least-squares fit to the data, indicating the hybrid DDIB-GO was dissolved homogeneously in the solvent.

applicability of Beer's law, from the slope of the linear least-squares fit we estimated the effective extinction coefficient of the DDIB-GO to be 0.0158 L mg⁻¹cm⁻¹ in ODCB at this position. The absorbance of solutions of DDIB-GO at other wavelengths was also consistent with the Beer's law. These results demonstrate that DDIB-GO has good solubility in ODCB.

Figure 7 is a typical AFM image of DDIB-GO dispersion in ODCB (0.1 mg mL⁻¹) after deposition on a freshly cleaved mica surface through drop-casting. The mica was dried at 60 °C in the vacuum for 12 hours, and was directly examined using atomic force microscope. Figure 7 shows a typical AFM image collected in the tapping mode displaying the morphology and thickness of the GO and DDIB-GO sheet. Individual GO sheets were imaged using AFM as shown in Figure 7(A). On average, the height of the GO sheets is ca. 0.87 nm with horizontal distance 20–200 nm, indicating that exfoliation of graphite down to individual GO nanosheets was indeed achieved.⁴² Figure 7(B) shows that sheets of different lateral dimensions between 20 and 200 nm, are mostly dispersed in single layer and the corresponding line-scan indicated that the average thickness of DDIB-GO was ca. 0.84 nm. The results were as expected that the functionalization on the edge of GO by small molecule did not change the size and thickness of GO sheets.

In order to further investigate the morphology of GO and DDIB-GO, TEM measurements have also been performed. The GO (in water) and DDIB-GO (in ODCB) dispersions of 0.1 mg mL⁻¹ were placed directly on two Cu grids and examined under TEM. Figure 8(A) shows that the materials of GO sheets that we used in the reaction were monolayer dispersed and was smooth and transparent. The TEM images of DDIB-GO (Fig. 8(B)) show that DDIB-GO are mostly single layers with few layers and small flakes stacked on top. Large graphitic domains are visible and distortions caused by the functional groups

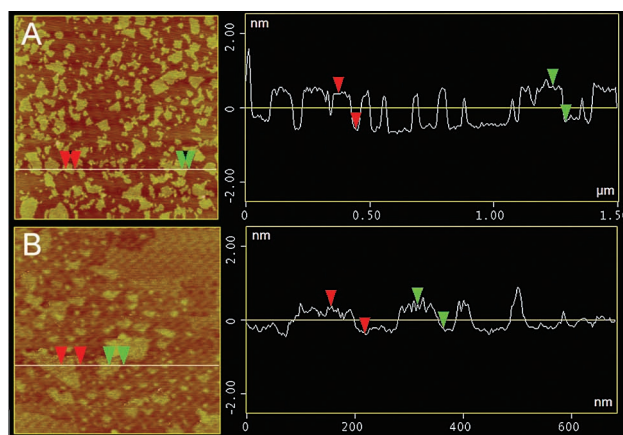


Fig. 7. AFM images and height profiles of (A) GO and (B) DDIB-GO sheets. Single sheets of DDIB-GO with an average thickness of about 0.8 nm are present, with different lateral dimensions between 20 and 200 nm.

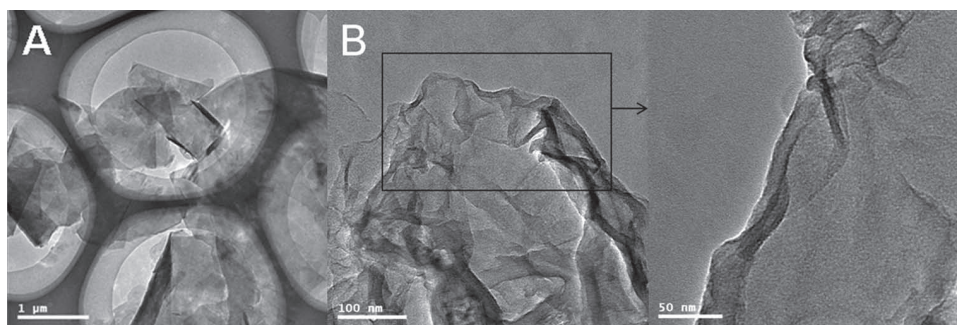


Fig. 8. TEM images of GO (A) and DDIB-GO (B). DDIB-GO is still monolayer dispersion with a wrinkled topology after functionalization.

and the extremely small thickness of the DDIB-GO sheets lead to a wrinkled topology. The morphology and well dispersion of the DDIB functionalized GO sheets obtained in this work are in agreement with the results as AFM images show. As expected, the images of AFM and TEM show that the size and shape of GO sheets have no obvious change after functionalization, which means that the functional groups have little effect on the morphology of GO sheets. And that is very important for further preparation of nanocomposite materials based on the GO or graphene.

The electrical conductivity of the as-prepared graphene films were measured at room temperature. At a given film thickness of ca. 40 nm, concomitant increase of film conductivity was observed with an increase in the heating temperatures from 300 to 1000 °C. As shown in Table I, the conductivity of film for DDIB increases with temperature ascending, which is attributed the content of graphite structure recovered. As the TGA spectra of DDIB-GO shown, the many epoxy, hydroxyl groups and adsorbed solvent molecule on the plane could be removed under 252 °C, so the conductivity of DDIB-GO ascends from insulator to 4.00×10^{-3} S/cm by thermal reduction at 300 °C. At 1000 °C, nearly all the functional groups on the GO are removed and the conjugated sp^2 network is largely restored. And due to the thermal fusion and surface-mediated reaction of graphene, it is reasonable to assume that the thermal annealing of the composite films consisting of graphene sheets and alkyl chains could heal the defects formed by oxide, so it shows high conductivity 823 S/cm, which is consistent with results reported.⁴⁴

Table I. Comparison of the dependence of sheet resistance and film (ca. 40 nm thickness) of DDIB-GO and conductivity for different reducing methods.

Graphene Films	Sheet Resistance (Ω/sq)	Film Conductivity (S/cm)
hydrazine + 300 °C	7.75×10^7	4.00×10^{-3}
hydrazine + 600 °C	1.73×10^5	1.65
hydrazine + 1000 °C	2.70×10^2	8.23×10^2

4. CONCLUSIONS

In summary, we have successfully developed a simple and fast method to obtain functionalized chemically converted graphene oxide nanosheets via the interaction of positive and negative charge with 1,3-didodecylimidazolium and the COO^- on the GO sheets. The results from FTIR, XPS, TGA, clearly indicated that the reaction between 1,3-didodecylimidazolium and the COO^- on the GO sheets occurred successfully. The AFM and TEM images show functionalized chemically converted graphene oxide flakes dispersed as single layer with crumpled silk waves have been obtained in this work. Homogeneous DDIB-GO sheets are well dispersed in ODCB, respectively, which would open up a wide range of possibilities for efficient chemical derivatization of GO or graphene where nonpolar media are required. It would also further broaden the scope of applications of GO or graphene, such as graphene-based organic and polymer composite materials or organic electronics utilizing graphene sheets as active layers. Finally, films cast from ODCB dispersions show good electrical conductivity, which would be used as electrode material.

Acknowledgments: The authors gratefully acknowledge financial support from the NSFC (Grants 50902073, 50933003 and 50903044), MOST (Grants 2011CB932602 and 2011DFB50300).

References and Notes

1. K. S. Novoselov, A. K. Geim, S. V. Morozov, D. Jiang, Y. Zhang, S. V. Dubonos, I. V. Grigorieva, and A. A. Firsov, *Science* 306, 666 (2004).
2. Y. B. Zhang, J. W. Tan, H. L. Stormer, and P. Kim, *Nature* 438, 201 (2005).
3. A. K. Geim and K. S. Novoselov, *Nat. Mater.* 6, 183 (2007).
4. X. L. Li, X. R. Wang, L. Zhang, S. Lee, and H. J. Dai, *Science* 319, 1229 (2008).
5. S. Stankovich, D. A. Dikin, G. H. B. Dommett, K. M. Kohlhaas, E. J. Zimney, E. A. Stach, R. D. Piner, S. T. Nguyen, and R. S. Ruoff, *Nat.* 442, 282 (2006).
6. S. Watcharotone, D. A. Dikin, S. Stankovich, R. Piner, I. Jung, G. H. B. Dommett, G. Evmenenko, S. E. Wu, S. F. Chen, C. P. Liu, S. T. Nguyen, and R. S. Ruoff, *Nano Lett.* 7, 1888 (2007).

7. T. Ramanathan, A. A. Abdala, S. Stankovich, D. A. Dikin, M. Herrera-Alonso, R. D. Piner, D. H. Adamson, H. C. Schniepp, X. Chen, R. S. Ruoff, S. T. Nguyen, I. A. Aksay, R. K. Prud'homme, and L. C. Brinson, *Nat. Nanotechnol.* 3, 327 (2008).
8. H. J. Jiang, *Small* 7, 2413 (2011).
9. X. Huang, Z. Y. Yin, S. X. Wu, X. Y. Qi, Q. Y. He, Q. C. Zhang, Q. Y. Yan, F. Boey, and H. Zhang, *Small* 7, 1876 (2011).
10. X. Huang, X. Y. Qi, F. Boey, and H. Zhang, *Chem. Soc. Rev.* 2012, DOI:10.1039/C1CS15078B.
11. X. Huang, S. Z. Li, Y. Z. Huang, S. X. Wu, X. Z. Zhou, S. Z. Li, C. L. Gan, F. Boey, C. A. Mirkin, and H. Zhang, *Nat. Commun.* 2, 292 (2011).
12. X. Huang, X. Z. Zhou, S. X. Wu, Y. Y. Wei, X. Y. Qi, J. Zhang, F. Boey and H. Zhang, *Small* 6, 513 (2010).
13. S. Gilje, S. Han, M. S. Wang, K. L. Wang, and R. B. Kaner, *Nano Lett.* 7, 3394 (2007).
14. X. Wang, L. J. Zhi, and K. Müllen, *Nano Lett.* 8, 323 (2008).
15. D. Li, M. B. Müller, S. Gilje, R. B. Kaner, and G. G. Wallace, *Nat. Nanotechnol.* 3, 101 (2008).
16. D. R. Dreyer, S. J. Park, C. W. Bielawski, and R. S. Ruoff, *Chem. Soc. Rev.* 39, 228 (2010).
17. X. Z. Zhou, X. Huang, X. Y. Qi, S. X. Wu, C. Xue, F. Y. C. Boey, Q. Y. Yan, P. Chen, and H. Zhang, *J. Phys. Chem. C* 113, 10842 (2009).
18. Y. Hernandez, V. Nicolosi, M. Lotya, F. M. Blighe, Z. Y. Sun, S. De, I. T. McGovern, B. Holland, M. Byrne, Y. K. Gun'Ko, J. J. Boland, P. Niraj, G. Duesberg, S. Krishnamurthy, R. Goodhue, J. Hutchison, V. Scardaci, A. C. Ferrari, and J. N. Coleman, *Nat. Nanotechnol.* 3, 563 (2008).
19. I. Jung, D. A. Dikin, R. D. Piner, and R. S. Ruoff, *Nano Lett.* 8, 4283 (2008).
20. Y. X. Xu, H. Bai, G. W. Lu, C. Li, and G. Q. Shi, *J. Am. Chem. Soc.* 130, 5856 (2008).
21. X. R. Wang, S. M. Tabakman, and H. J. Dai, *J. Am. Chem. Soc.* 130, 8152 (2008).
22. Q. H. Wang and M. C. Hersam, *Nat. Chem.* 1, 206 (2009).
23. X. Y. Qi, K.-Y. Pu, H. Li, X. Z. Zhou, S. X. Wu, Q.-L. Fan, B. Liu, F. Boey, W. Huang, and H. Zhang, *Angew. Chem. Int. Ed.* 49, 9426 (2010).
24. X. Y. Qi, K.-Y. Pu, X. Z. Zhou, H. Li, B. Liu, F. Boey, W. Huang, and H. Zhang, *Small* 6, 663 (2010).
25. S. Wang, P.-J. Chia, L.-L. Chua, L.-H. Zhao, R.-Q. Png, S. Sivaramakrishnan, M. Zhou, R. G.-S. Goh, R. H. Friend, A. T.-S. Wee, and P. K.-H. Ho, *Adv. Mater.* 20, 3440 (2008).
26. H. F. Yang, C. S. Shan, F. H. Li, D. X. Han, Q. X. Zhang, and L. Niu, *Chem. Commun.* 3880 (2009).
27. X. M. Sun, Z. Liu, K. Welscher, J. T. Robinson, A. Goodwin, S. Zaric, and H. J. Dai, *Nano Res.* 1, 203 (2008).
28. M. Fang, K. G. Wang, H. B. Lu, Y. L. Yang, and S. Nuttb, *J. Mater. Chem.* 19, 7098 (2009).
29. E. Bekyarova, M. E. Itkis, P. Ramesh, C. Berger, M. Sprinkle, W. A. de Heer, and R. C. Haddon, *J. Am. Chem. Soc.* 131, 1336 (2009).
30. C. E. Hamilton, J. R. Lomeda, Z. Z. Sun, J. M. Tour, and A. R. Barron, *Nano Lett.* 9, 3460 (2009).
31. S. Niyogi, E. Bekyarova, M. E. Itkis, J. L. McWilliams, M. A. Hamon, and R. C. Haddon, *J. Am. Chem. Soc.* 128, 7720 (2006).
32. W. J. Hong, Y. X. Xu, G. W. Lu, C. Li, and G. Q. Shi, *Electrochemistry Comm.* 10, 1555 (2008).
33. M. Lotya, Y. Hernandez, P. J. King, R. J. Smith, V. Nicolosi, L. S. Karlsson, F. M. Blighe, S. De, Z. M. Wang, I. T. McGovern, G. S. Duesberg, and J. N. Coleman, *J. Am. Chem. Soc.* 131, 3611 (2009).
34. K. P. Loh, Q. L. Bao, P. K. Ang, and J. X. Yang, *J. Mater. Chem.* 20, 2277 (2010).
35. Y. Y. Liang, D. Q. Wu, X. L. Feng, and K. Müllen, *Adv. Mater.* 21, 1679 (2009).
36. T. Y. Kim, H. W. Lee, J. E. Kim, and K. S. Suh, *ACS. Nano* 4, 1612 (2010).
37. W. S. Hummers, JR., and R. E. Offeman, *J. Am. Chem. Soc.* 80, 1339 (1958).
38. A. Getsis, B. Balke, C. Felser, and A.-V. Mudring, *Cryst. Growth Des.* 9, 4429 (2009).
39. Y. S. Vygodskii, E. I. Lozinskaya, and A. S. Shaplov, *Macromol. Rapid Commun.* 23, 676 (2002).
40. S. Stankovich, R. D. Piner, S. T. Nguyen, and R. S. Ruoff, *Carbon* 44, 3342 (2006).
41. C. Vallés, C. Drummond, H. Saadaoui, C. A. Furtado, M. He, O. Roubeau, L. Ortolani, M. Monthieux, and A. Pénicaud, *J. Am. Chem. Soc.* 130, 15802 (2008).
42. S. Stankovich, D. A. Dikin, R. D. Piner, K. A. Kohlhaas, A. Kleinhammes, Y. Y. Jia, Y. Wu, S. T. Nguyen, and R. S. Ruoff, *Carbon* 45, 1558 (2007).
43. Z. Guo, F. Du, D. Ren, Y. S. Chen, J. Y. Zheng, Z. B. Liu, and J. G. Tian, *J. Mater. Chem.* 16, 3021 (2006).
44. H. A. Becerril, J. Mao, Z. F. Liu, R. M. Stoltenberg, Z. N. Bao, and Y. S. Chen, *ACS Nano* 2, 463 (2008).

Received: 6 September 2011. Accepted: 31 October 2011.